THE ASTROPHYSICAL JOURNAL, 438:527–538, 1995 January 10

OPTICAL RADII OF GALAXY CLUSTERS

M. GIRARDI,[1,2] A. BIVIANO,[3] G. GIURICIN,[1,2] F. MARDIROSSIAN,[1,2] AND M. MEZZETTI[1,2]
Received 1994 February 22; accepted 1994 July 5

ABSTRACT

We analyze the density profiles and virial radii for a sample of 90 nearby clusters, using galaxies with available redshifts and positions. Each cluster has at least 20 redshifts measured within an Abell radius, and all the results come from galaxy sets of at least 20 members.

Most of the density profiles of our clusters are well fitted by hydrostatic isothermal-like profiles. The slopes we find for many cluster density profiles are consistent with the hypothesis that the galaxies are in equilibrium with the binding cluster potential.

The virial radii correlate with the core radii at a very high significance level. The observed relationship between the two size estimates is in agreement with the theoretical one computed by using the median values of the density profile parameters fitted on our clusters.

After correcting for incompleteness in our cluster sample, we provide the universal distribution functions of core and virial radii (obtained within half an Abell radius).

Subject headings: galaxies: clusters: general

1. INTRODUCTION

The distribution functions of observational cluster quantities, such as radii, velocity dispersions, masses, luminosities, and X-ray temperatures, can provide strong constraints both on cosmological scenarios and on the internal dynamics of these systems. Theoretical as well as observational estimates of these distribution functions are presently being debated.

In previous papers (Girardi et al. 1993, hereafter GBGMM; Biviano et al. 1993), we have addressed the distributions of cluster velocity dispersions and virial masses. Here we deal with the spatial distribution of member galaxies in clusters. Existing relations between the linear sizes and other physical quantities of bound systems of galaxies have been investigated in the literature, both observationally and theoretically (see, e.g., Oemler 1974; Bahcall 1975; Peebles 1976; Dressler 1978; Sarazin 1980; Giuricin, Mardirossian, & Mezzetti 1984; West, Dekel, & Oemler 1987; West, Oemler, & Dekel 1989; Peebles, Daly, & Juszkiewicz 1989; Lilje & Lahav 1991; Cavaliere, Colafrancesco, & Scaramella 1991; Edge & Stewart 1991; Inagaki, Itoh, & Saslaw 1992; Kashlinsky 1992; and references therein).

Several size estimates are present in the literature: the core radius, the effective radius, the virial radius, the harmonic radius, the gravitational radius, the mean radius, and so forth (see, e.g., Bahcall 1977, and references therein). In the present paper we deal with virial and core radii.

Relaxation processes naturally lead to the formation of physical cores in clusters of galaxies (see, e.g., King 1966; Lynden-Bell 1967; Peebles 1970; Sarazin 1986). In general, in order to fit the galaxy distribution of clusters, the following surface density profile has been assumed (see, e.g., Bahcall 1977; Sarazin 1980; and references therein):

$$\sigma(r) = \frac{\sigma_0}{[1 + (r/R_c)^2]^\alpha}\,, \qquad (1)$$

where σ_0 is the *central projected galaxy density* and R_c is the *core radius*. This model corresponds for $r \gg R_c$ to a *volume density* $\rho(r) \propto r^{-2\alpha-1}$. Many authors (see, e.g., Bahcall 1975; Dressler 1978; Sarazin 1986) have used the King (1962) model to fit the cluster profiles; this corresponds to the model of equation (1) with $\alpha = 1$. For instance, Bahcall (1975) found an average value of *King* $R_c \simeq 0.12 \pm 0.02\ h^{-1}$ Mpc (the Hubble constant is $H_0 = 100\ h$ km s^{-1} Mpc^{-1}) on a sample of 15 rich regular clusters; in contrast, Dressler (1978) found an average value of King $R_c \simeq 0.24 \pm 0.06\ h^{-1}$ Mpc on another sample of 12 clusters. From the large compilation by Sarazin (1986), it may be noted that very different values of King R_c for the same cluster have been obtained by different authors.

Core radii have also been derived from the X-ray surface brightness distributions, by fitting these profiles to hydrostatic isothermal models (see, e.g., Abramopoulous & Ku 1983; Jones & Forman 1984; Lubin & Bahcall 1993; Bahcall & Lubin 1993; and references therein). An average value of $\sim$0.05–0.15 h^{-1} Mpc is suggested for X-ray core radii, although both smaller (Durret et al. 1994) and larger (Jones & Forman 1992) values have been found.

Attempts to evaluate the core radius of the cluster dark matter component have been made (see, e.g., Eyles et al. 1991; Gerbal et al. 1992; Kneib et al. 1993; Miralda-Escudé 1992; Soucail 1992). The results are still preliminary.

In this paper we use the hydrostatic isothermal models in other to fit the cluster density profiles. In particular, this choice is corroborated by the recent results of Bahcall & Lubin (1993; see also Gerbal, Durret, & Lachièze-Rey 1994), who claim that the "β-discrepancy" can be solved by fitting the galaxy density profiles with models having $\alpha = 0.7 \pm 0.1$ in equation (1), i.e., $\rho(r) \propto r^{-2.4\pm0.2}$ at large values of r, instead of using the classical King models. We recall that the β-discrepancy is the difference between the observed values of $\beta_{\rm spec}$, determined from cluster X-ray temperatures and velocity dispersions, and $\beta_{\rm fit}$, determined from the gas and the galaxy density profiles in galaxy clusters (see, e.g., Sarazin 1986).

The *virial radius* has been extensively used in the literature to evaluate the size and masses (via the virial theorem) of galaxy systems (see, e.g., Limber & Matthews 1960; Smith 1980;

[1] Scuola Internazionale Superiore di Studi Aranzati (SISSA), via Beirut 4, 34013 Trieste, Italy; girardi,giuricin,mardirossian,mezzetti@tsmi19.sissa.it.
[2] And Dipartimento di Astronomia, Università degli Studi di Trieste.
[3] Institut d'Astrophysique de Paris, 98 bis, Boulevard Arago, 75014 Paris, France; biviano@iap.fr.

Fernley & Bhavsar 1984; West et al. 1989; Perea, del Olmo, & Moles 1990; Pisani et al. 1992; Biviano et al. 1993). In the present paper we consider the two-dimensonal projected virial radius (i.e., not deprojected by the classical value of $\pi/2$),

$$R_v = \frac{N^2}{\sum_{i,j=1}^{N} R_{ij}^{-1}}, \qquad (2)$$

where N is the number of cluster members and R_{ij} is the projected distance between the i and the j members.

In this framework, we deemed it interesting to obtain estimates of cluster sizes using a large data sample of 90 clusters, and we examine the relationships between these sizes and other cluster properties. In § 2 we describe our data sample; in § 3 we consider the method of analysis; in § 4 we provide the results and the relevant discussion; and in § 5 we list our conclusions.

2. THE DATA SAMPLE

We based our analysis on a sample of 90 nearby ($z < 0.15$) clusters, each one with at least 20 measured redshifts of cluster members within 1.5 h^{-1} Mpc. In this compilation we included some poor clusters (or rich groups) in order to enlarge our range of cluster richness.

The problem of foreground and background contamination may be severe when redshift information is not available for all the galaxies considered. In fact, different correlations have been adopted in the literature, leading to very different estimates for the sizes of the same clusters (see, e.g., Bahcall 1975; Dressler 1978; Fitchett & Merritt 1988; West et al. 1987).

On the contrary, using observed redshifts and positions for all our cluster galaxies, we have been able to assign the cluster membership. Therefore, our sample should be considered quite free from contamination. The procedure adopted to reject non–cluster members is similar to that described in GBGMM. However, in this paper we have decided to adopt a somewhat stricter selection criterion, which is described below.

In order to reject interlopers in the clusters, we make use of the distance of a galaxy from the cluster center in the coordinates and in the velocity space. The center is defined as a biweighted mean of the velocities, right ascensions, and declinations (see, e.g., Beers, Flynn, & Gebhardt 1990; GBGMM).

A first selection is performed to separate obvious groups which are projected in the same cluster field. First, we identify all groups separated by a weighted gap larger than four in the velocity space. A weighted gap in the space of the ordered velocities is defined as the difference between two contiguous velocities, weighted according to their rank in the ordered distributions: the closer to the center of the distribution the gap, the higher its weight (for further details see, e.g., Beers et al. 1990). We then select as our cluster the larger of these groups. Of the remaining galaxies, we subsequently reject all of them lying outside a circle of 3 h^{-1} Mpc from the cluster center. This rejection is made in an iterative way, recomputing the center after each iteration and thus redefining the 3 h^{-1} Mpc circle and the rejected galaxies, until convergence is reached.

This defines the main cluster body. Further selection requires the exclusion of galaxies more distant than 4000 km s^{-1} from the cluster mean velocity (as in Beers et al. 1991; GBGMM) and further rejection of galaxies separated from the main cluster body by a weighted gap larger than four in the velocity space. The greatest difference with respect to GBGMM is in the last selection in the coordinate space: we reject all galaxies more distant than 1.5 h^{-1} Mpc from the cluster center, once again in an iterative way. Since the size estimators are not as robust as the estimators of velocity dispersions used in GBGMM, we believe that restricting the analysis to galaxies within 1.5 h^{-1} Mpc is a very simple but efficient method to reduce the problem of interlopers, since the higher the aperture, the larger the ratio between background/foreground galaxies and cluster members. Thus it is more conservative to consider the inner cluster regions.

Problems of magnitude incompleteness may cause errors in the size estimates (e.g., Dressler 1978). In particular, if a deeper sampling of galaxies (in terms of magnitudes) has been made by observers in the central regions, the shape of the density profile will look steeper than it is in reality. We have therefore analyzed all our clusters with available galaxy magnitudes, by looking at the galaxy magnitudes as a function of clustercentric distance. We have noted that some clusters are sampled more deeply close to the center than they are outside. We have rejected the fainter galaxies of these clusters so as to erase any trend of the limiting magnitude with clustercentric distance.

Yet another sort of bias may be present if some regions in the cluster are not covered observationally (generally, in the outer parts). As for the previous case, the shape of the density profile will look artifically steeper than it is in reality. There is no easy way to eliminate this sort of bias a priori, but a signature of it may be the steepening of the density profile with increasing apertures. As a consequence, we look with more confidence on those results obtained from the central regions of our clusters, where problems of incompleteness should not be so strong (see § 3).

Yet another problem is the presence of substructures which may bias the determination of cluster sizes, and in particular of the core radii (see, e.g., Sarazin 1980). When the cluster has several density clumps, one density profile might not adequately fit the galaxy distribution; large, spurious values of the core radius are expected when a single profile is forced to fit all the data. In order to investigate the possible presence of subclustering in our sample, we performed the test of Dressler & Schectman (1988b). This test gives the probability, $1 - P_{DS}$, that some subclustering exists in the cluster (1000 simulations were run, according to the prescriptions of the above-mentioned authors). Actually this method like others available in the literature) is not efficient when the number of galaxies considered is low ($N < 40$). As a consequence , we considered the subsample of our clusters, with $N \geq 40$ members and no evidence of subclustering, in order to check our results. As detailed in § 4, our results do not seem to be biased by subclustering.

The sample of the 90 clusters considered is listed in Table 1, together with the number N of galaxy members inside 1.5 h^{-1} Mpc from the cluster center, the Abell number counts (C), the richness class (R), the Bautz-Morgan and the Rood-Sastry classes (BM type and RS type), the probability P_{DS} that observed structures in the cluster are chance fluctuations (i.e., low values of P_{DS} indicate a high probability of subclustering), and the relevant reference sources for velocities.

3. THE METHOD OF ANALYSIS

In order to obtain the values of R_c, we fitted the observed galaxy distributions to hydrostatic isothermal models on the hypothesis of spherical symmetry. Although clusters are not spherically symmetric (their flattening may indeed be quite large, see, e.g., Rhee, van Haarlem, & Katgert 1992), we prefer not to include ellipticity as a free parameter in our fits because

TABLE 1

CLUSTER PROPERTIES

Name (1)	N (2)	C (3)	R (4)	BM Type (5)	RS Type (6)	P_{DS} (7)	Reference (8)
ACO 85	121	59	1	I	cD	0.29	1
ACO 119	77	69	1	II/III	C	0.01	2
ACO 151	31	72	1	II	cD	...	3
ACO 193	56	58	1	I	cD	0.61	4
ACO 194	59	37	0	II	L	0.16	5
ACO 262	45	40	0	III	C	0.24	6, 7, 8
ACO 399	100	57	1	I/II	cD	0.27	4
ACO 400	88	58	1	II/III	I	0.03	9
ACO 401	106	90	2	I	cD	0.53	4
ACO 426/Perseus	93	88	2	II/III	L	0.69	10
ACO 458	32	114	2	I/II	cD	...	11
ACO 496	41	50	1	I	cD	0.19	12
ACO 539	82	50	1	III	F	0.33	13
ACO 548	126	79	1	III	F	0.00	14
ACO 576	41	61	1	III	I	0.93	15
ACO 634	35	40	0	III	F	...	16
ACO 744	21	42	0	II	C	...	17
ACO 754	68	92	2	I/II	cD	0.78	14
ACO 779	22	32	0	I/II	cD	...	18, 19
ACO 957	31	55	1	I/II	L	...	20
ACO 999	24	33	0	II/III	L	...	21
ACO 1016	22	37	0	...	L	...	21
ACO 1060/Hydra	131	50	1	III	C	0.00	22, 23
ACO 1142	40	35	0	II/III	C	0.36	24
ACO 1146	60	222	4	I	cD	0.16	25
ACO 1185	29	52	1	II	C	...	20
ACO 1367	69	117	2	II/III	F	0.10	26, 27, 28, 29
ACO 1631	59	34	0	I	C	0.09	14
ACO 1644	82	68	1	II	cD	0.10	14
ACO 1651	29	70	1	I/II	cD	...	18
ACO 1656/Coma	180	106	2	II	B	0.36	30
ACO 1736	34	...	...	...	...	...	14
ACO 1736	55	...	...	...	...	0.02	14
ACO 1750	47	40	0	II/III	F	0.00	20
ACO 1795	83	115	2	I	cD	0.48	4
ACO 1809	52	78	1	II	cD	0.07	4
ACO 1983	69	51	1	III	F	0.29	14
ACO 1991	25	60	1	I	F	...	20
ACO 2029	35	82	2	I	cD	...	31, 32
ACO 2052	41	41	0	I/II	cD	0.89	33
ACO 2063	65	63	1	II	cD	0.38	4, 20
ACO 2079	26	57	1	II/III	cD	...	34
ACO 2107	68	51	1	I	cD	0.00	35
ACO 2124	66	50	1	I	cD	0.67	4
ACO 2147−2152	39	...	...	III	...	...	36
ACO 2151/Hercules	96	87	2	III	F	0.00	14
ACO 2197	41	73	1	III	L	0.00	37
ACO 2199	32	88	2	I	cD	...	37
ACO 2255	29	102	2	II/III	C	...	38
ACO 2256	86	88	2	II/III	B	0.20	39
ACO 2319A	22	...	...	...	...	...	31
ACO 2440	24	32	0	II	L	...	20
ACO 2538	38	72	1	II/III	C	...	11
ACO 2554	28	159	3	II	L	...	11
ACO 2589	33	40	0	I	cD	...	20
ACO 2593	37	42	0	II	F	...	20
ACO 2670	196	142	3	I/II	cD	0.01	40
ACO 2717	33	52	1	I/II	...	...	11
ACO 2721	63	192	3	II	L	0.39	25
ACO 2877	97	30	0	I	cD	0.04	1
ACO 3266	130	91	2	I/II	cD	0.31	25
ACO 3334	32	82	2	I/II	...	...	11
ACO 3360	37	85	2	III	...	...	11
ACO 3376	69	42	0	I	...	0.14	14
ACO 3381	30	69	1	I	...	...	14
ACO 3389	39	35	0	II/III	C	...	25
ACO 3391	65	40	0	I	cD	0.02	25
ACO 3395	146	54	1	II	C	0.01	25
ACO 3526/Centaurus	109	33	0	I/II	I	0.02	41, 42
ACO 3532	43	36	0	II/III	...	0.19	43
ACO 3558	113	226	4	I	cD	0.10	25, 44

TABLE 1—*Continued*

Name (1)	N (2)	C (3)	R (4)	BM Type (5)	RS Type (6)	P_{DS} (7)	Reference (8)
ACO 3574	38	31	0	I	...	...	45
ACO 3667	105	85	2	I/II	L	0.53	46
ACO 3705	40	100	2	III	...	0.38	11
ACO 3716	79	66	1	I/II	...	0.16	14
ACO 3854	36	130	3	II	...	...	11
ACO 4067	29	72	1	III	F	...	25
AWM 1	25	...	0	II/III	...	...	47
Cancer	58	...	...	...	...	0.03	48
DC 0003−50	36	...	...	...	...	...	14
Eridanus	54	...	...	...	...	0.04	49
MKW 4	43	...	0	I	cD	0.01	47, 50
Pegasus I	43	...	0	II	...	0.05	51, 52, 53
ACO S301	24	5	0	I	...	...	14
ACO S373/Fornax	56	−18	0	I	...	0.03	42
ACO S463	81	26	0	I/II	...	0.00	14
S753	34	18	0	I	...	...	45
ACO S805	25	8	0	I	...	...	54
Ursa Major	57	...	...	...	...	0.01	55
Virgo	362	...	1	III	I	0.00	56

REFERENCES.—(1) Malumuth et al. 1992; (2) Fabricant et al. 1993; (3) Proust et al. 1992; (4) Hill & Oegerle 1993; (5) Chapman, Geller, & Huchra 1988; (6) Giovanelli, Haynes, & Chincarini 1982; (7) Gregory, Thompson, & Tifft 1981; (8) Moss & Dickens 1977; (9) Beers et al. 1992; (10) Kent & Sargent 1983; (11) Colless & Hewett 1987; (12) Quintana & Ramirez 1990; (13) Ostriker et al. 1988; (14) Dressler & Shectman 1988s; (15) Hintzen et al. 1982; (16) Stepanyan 1984; (17) Kurtz et al. 1985; (18) Zabludoff, Huchra, & Geller 1990; (19) Hintzen, Oegerle, & Scott 1978; (20) Beers et al. 1991; (21) Chapman, Geller, & Huchra 1987; (22) Richter 1987; (23) Richter 1989; (24) Geller et al. 1984; (25) Teague, Carter, & Gray 1990; (26) Gavazzi 1987; (27) Gregory & Thompson 1978; (28) Tifft 1978; (29) Dickens & Moss 1976; (30) Kent & Gunn 1982; (31) Faber & Dressler 1977; (32) Bowers, Ellis, & Efstathiou 1988; (33) Quintana et al. 1985; (34) Postman, Huchra, & Geller 1986; (35) Oegerle & Hill 1993; (36) Tarenghi et al. 1979; (37) Gregory & Thompson 1984; (38) Stauffer, Spinrad, & Sargent 1979; (39) Fabricant, Kent, & Kurtz 1989; (40) Sharples, Ellis, & Gray 1988; (41) Dickens, Currie, & Lucey 1986; (42) Lauberts & Valentjin 189; (43) Cristiani et al. 1987; (44) Metcalfe, Godwin, & Spenser 1987; (45) Willmer et al. 1991; (46) Sodrè et al. 1992; (47) Beers et al. 1984; (48) Bothum et al. 1983; (49) Willmer et al. 1989; (50) Malumuth & Kriss 1986; (51) Richter & Huchtmeier 1982; (52) Bothun et al. 1985; (53) Chincarini & Rood 1976; (54) Bell & Whitmore 1989; (55) Tully 1988; (56) Binggeli, Sandage, & Tammann 1985.

it would be poorly constrained in many clusters of our data set, where we do not have enough data, and because inhomogeneous sampling during observing may result in artificial shapes for some clusters. We nonetheless performed Monte Carlo realizations of distributions of 25, 50, 100, and 200 points extracted from King density profiles with varying R_c and ellipticity, and we analyzed how the derived values of R_c depend on the assumption of spherical symmetry. Not surprisingly, these values are intermediate between the values of the major-axis and minor-axis core radii, and consistent with both within the formal errors. Therefore, we think that the assumption of spherical symmetry is a good working hypothesis.

The fitting was performed using the maximum likelihood technique, which takes directly into account the positions of individual galaxies and does not require any binning of the data (see, e.g., Sarazin 1980). This method is very efficient since it does not introduce any artificial scales, and it allows the simultaneous fitting of R_c and α. On the basis of the discussion of the previous section about interlopers, we assumed that the background galaxy density was negligible, and we set it at zero.

We allowed R_c and α to vary from 0 to 1 and from 0.5 to 1.5, respectively; we rejected values of R_c larger than 1 h^{-1} Mpc and values of α outside the above-mentioned interval. Moreover, we did not consider size estimates for clusters whose fitted profiles are rejected by a Kolmogorov-Smirnov (K-S) test at 90% probability. However, fitting both R_c and α at the same time is not an easy task, especially when the data set is poor. In a second stage of the investigation (see § 4), we therefore decided to fix the value of α at the median value obtained in the two-parameter fitting procedure. By reducing the free parameters to one, R_c, we were able to better constrain the size estimates.

The errors on our R_c were estimated by following the prescriptions of Avni (1976), while the errors on our R_v were obtained via the "jackknife" technique (see, e.g., Efron 1979; Geller 1984).

4. CORE AND VIRIAL RADII

We obtained both the virial radii and the best fits of cluster profiles with three increasing apertures, i.e., 0.5. 0.75, and 1 h^{-1} Mpc.

In Table 2 we give the virial radii for our sample of clusters: in column (1) we list the cluster name; in columns (2), (3), and (4) we give values of $R_{v,0.5}$, $R_{v,0.75}$, and $R_{v,1}$, and their errors, computed within the increasing apertures 0.5, 0.75, and 1 h^{-1} Mpc for each cluster (if at least 20 members are contained within the respective aperture).

In Table 3 we give the median values of the core radii, $R_{c,0.5}$, $R_{c,0.75}$, and $R_{c,1}$, and of the α's, $\alpha_{0.5}$, $\alpha_{0.75}$, and α_1, for our clusters, computed within the apertures of 0.5, 0.75, and 1 h^{-1} Mpc, respectively. The numbers of cluster fittings, the core radii, and the values of α are listed in columns (1), (2), and (3). The fittings were performed only if at last 20 members are contained within the respective aperture. Only the *good* fits were considered (see § 3).

The fitted profiles seem to be steeper when apertures larger than 0.50 h^{-1} Mpc are considered. This trend may be explained either by sampling incompleteness or by a true dif-

TABLE 2

CLUSTER VIRIAL RADII

Name (1)	$R_{v,0.50}$ (2)	$R_{v,0.75}$ (3)	$R_{v,1.00}$ (4)
ACO 85	0.58 ± 0.05	0.78 ± 0.05	0.93 ± 0.05
ACO 119	0.47 ± 0.04	0.71 ± 0.06	0.87 ± 0.07
ACO 151	...	0.39 ± 0.09	0.46 ± 0.10
ACO 193	0.42 ± 0.03	0.54 ± 0.05	...
ACO 194	0.47 ± 0.06	0.60 ± 0.07	0.69 ± 0.08
ACO 262	0.46 ± 0.07	0.62 ± 0.10	0.85 ± 0.12
ACO 399	0.64 ± 0.03	0.83 ± 0.04	1.05 ± 0.06
ACO 400	0.51 ± 0.04	0.69 ± 0.06	0.78 ± 0.06
ACO 401	0.51 ± 0.04	0.73 ± 0.05	0.91 ± 0.06
ACO 426/Perseus	0.45 ± 0.03	0.55 ± 0.05	0.67 ± 0.06
ACO 458	0.54 ± 0.05	...	...
ACO 496	0.62 ± 0.05	0.77 ± 0.06	...
ACO 539	0.43 ± 0.05	0.59 ± 0.07	0.65 ± 0.08
ACO 548	...	0.94 ± 0.05	1.01 ± 0.07
ACO 576	0.46 ± 0.04	...	...
ACO 634	...	0.76 ± 0.09	0.91 ± 0.10
ACO 744	0.35 ± 0.07	0.35 ± 0.07	...
ACO 754	0.57 ± 0.05	0.67 ± 0.04	0.85 ± 0.07
ACO 779	...	...	0.77 ± 0.19
ACO 957	0.39 ± 0.04	...	...
ACO 999	...	0.58 ± 0.09	...
ACO 1016	0.45 ± 0.07	...	...
ACO 1060/Hydra	0.49 ± 0.04	0.69 ± 0.05	0.81 ± 0.05
ACO 1142	...	0.89 ± 0.06	0.94 ± 0.07
ACO 1146	0.61 ± 0.04	0.68 ± 0.05	0.74 ± 0.06
ACO 1185	0.30 ± 0.03	0.41 ± 0.07	0.41 ± 0.07
ACO 1367	0.50 ± 0.04	0.63 ± 0.05	...
ACO 1631	0.53 ± 0.07	0.75 ± 0.07	0.86 ± 0.08
ACO 1644	0.67 ± 0.03	0.83 ± 0.05	1.00 ± 0.07
ACO 1651	...	0.56 ± 0.11	...
ACO 1656/Coma	0.47 ± 0.03	0.57 ± 0.03	0.75 ± 0.05
ACO 1736	...	...	1.19 ± 0.13
ACO 1736	0.60 ± 0.07	0.79 ± 0.06	0.95 ± 0.08
ACO 1750	0.40 ± 0.06	0.51 ± 0.05	0.57 ± 0.06
ACO 1795	0.42 ± 0.05	0.65 ± 0.07	0.83 ± 0.09
ACO 1809	0.51 ± 0.04	0.60 ± 0.05	0.66 ± 0.06
ACO 1983	0.47 ± 0.07	0.61 ± 0.08	0.80 ± 0.09
ACO 1991	0.35 ± 0.03	...	...
ACO 2029	0.24 ± 0.04	...	...
ACO 2052	0.53 ± 0.06	0.65 ± 0.07	0.67 ± 0.07
ACO 2063	0.42 ± 0.04	0.56 ± 0.06	0.61 ± 0.07
ACO 2079	...	...	1.07 ± 0.18
ACO 2107	0.46 ± 0.04	0.60 ± 0.06	...
ACO 2124	0.56 ± 0.04	0.66 ± 0.05	0.77 ± 0.06
ACO 2147−2152	...	...	1.13 ± 0.12
ACO 2151/Hercules	0.57 ± 0.04	0.80 ± 0.05	0.99 ± 0.06
ACO 2197	0.57 ± 0.09	0.70 ± 0.09	0.90 ± 0.12
ACO 2199	...	...	0.88 ± 0.13
ACO 2255	...	0.46 ± 0.08	0.63 ± 0.12
ACO 2256	0.51 ± 0.04	0.64 ± 0.05	0.81 ± 0.06
ACO 2319A	...	0.56 ± 0.10	...
ACO 2440	0.45 ± 0.06	...	...
ACO 2538	0.50 ± 0.06	0.66 ± 0.08	...
ACO 2554	0.60 ± 0.04	...	...
ACO 2589	0.32 ± 0.03	...	...
ACO 2593	0.39 ± 0.04	0.39 ± 0.04	0.39 ± 0.04
ACO 2670	0.47 ± 0.03	0.63 ± 0.04	0.77 ± 0.05
ACO 2717	0.45 ± 0.05	0.54 ± 0.07	...
ACO 2721	0.61 ± 0.05	0.80 ± 0.07	0.91 ± 0.07
ACO 2877	0.47 ± 0.03	0.52 ± 0.04	0.55 ± 0.04
ACO 3266	0.49 ± 0.05	0.77 ± 0.05	0.98 ± 0.05
ACO 3334	0.49 ± 0.05	...	...
ACO 3360	0.51 ± 0.04	...	...
ACO 3376	0.54 ± 0.04	0.67 ± 0.05	0.77 ± 0.07
ACO 3381	...	0.61 ± 0.07	0.70 ± 0.08
ACO 3389	0.45 ± 0.05	...	...
ACO 3391	0.52 ± 0.06	0.72 ± 0.06	...
ACO 3395	0.52 ± 0.03	0.76 ± 0.04	0.84 ± 0.05
ACO 3526/Centaurus	0.52 ± 0.03	0.68 ± 0.04	0.81 ± 0.05
ACO 3532	0.54 ± 0.07	...	...
ACO 3558	0.45 ± 0.03	0.60 ± 0.04	...
ACO 3574	0.60 ± 0.06	0.79 ± 0.07	0.89 ± 0.09
ACO 3667	0.52 ± 0.07	0.78 ± 0.07	1.02 ± 0.07
ACO 3705	0.61 ± 0.05	0.67 ± 0.05	...
ACO 3716	0.51 ± 0.04	0.65 ± 0.05	0.74 ± 0.06
ACO 3854	0.62 ± 0.05	0.74 ± 0.06	...
ACO 4067	...	0.70 ± 0.10	0.82 ± 0.10
AWM 1	...	...	0.74 ± 0.14
Cancer	0.49 ± 0.07	0.67 ± 0.08	0.81 ± 0.10
DC 0003−50	...	0.71 ± 0.07	0.83 ± 0.10
Eridanus	...	0.86 ± 0.07	1.05 ± 0.07
MKW 4	0.41 ± 0.05	0.47 ± 0.06	0.51 ± 0.07
Pegasus I	...	0.58 ± 0.08	0.72 ± 0.10
ACO S301	...	0.53 ± 0.10	0.63 ± 0.13
ACO S373/Fornax	0.49 ± 0.08	0.72 ± 0.07	0.86 ± 0.09
ACO S463	0.48 ± 0.03	0.65 ± 0.05	0.82 ± 0.07
S753	0.52 ± 0.10	0.73 ± 0.11	...
ACO S805	...	...	0.66 ± 0.15
Ursa Major	...	0.94 ± 0.08	1.10 ± 0.08
Virgo	0.54 ± 0.03	0.74 ± 0.03	1.06 ± 0.03

ference between the profiles of the inner and the outer cluster regions (see, e.g., Bahcall & Lubin 1993). When we restrict our analysis of the inner regions, we note that the distributions of $\alpha_{0.5}$ and $\alpha_{0.75}$ do not differ significantly, according to the K-S and sign tests; the same holds for $R_{c,0.5}$ and of $R_{c,0.75}$. The profiles seem to be well defined within 0.75 h^{-1} Mpc; therefore, we restricted our analysis to this inner region.

Fixing the α-parameter in the fitting procedure makes it possible to reduce the formal errors on the derived values of

TABLE 3

PROFILE PARAMETERS

No. of Fits (1)	R_c (2)	α (3)
29	$R_{c,0.50} = 0.11^{+0.03}_{-0.04}$	$\alpha_{0.50} = 0.8^{+0.3}_{-0.1}$
30	$R_{c,0.75} = 0.12^{+0.08}_{-0.06}$	$\alpha_{0.75} = 0.9^{+0.2}_{-0.1}$
26	$R_{c,1.00} = 0.16^{+0.04}_{-0.09}$	$\alpha_{1.00} = 0.9^{+0.3}_{-0.1}$

the core radii. Our median value of $\alpha_{0.5}$ is $0.8^{+0.3}_{-0.1}$. It does not differ, within the errors, from 0.7 ± 0.1, which is the α-value suggested by Bahcall & Lubin (1993; see also Bahcall 1977) to resolve the β-discrepancy for clusters of galaxies. So, we chose the value of 0.8 in our α-fixed models.

In Table 4 we list the core radii obtained with the fixed $\alpha = 0.8$ profiles: in column (1) we list the cluster name; in column (2) we list the values of $R_{c,0.5,\alpha=0.8}$ and their errors, computed within the aperture of 0.5 h^{-1} Mpc, and in column (3) the corresponding confidence levels (in percent) $P_{0.5,\alpha=0.8}$ of the profile fittings (obtained by using the K-S test); in column (4) we list the values of $R_{c,0.75,\alpha=0.8}$ and their errors, computed within the aperture of 0.75 h^{-1} Mpc, and in column (5) the corresponding confidence levels (in percent) $P_{0.75,\alpha=0.8}$ of the profile fittings (obtained by using the K-S test).

As usual, the fits were performed only on samples with at least 20 galaxies contained with the aperture considered.

The median values and the distributions of $R_{c,0.5,\alpha=0.8}$ and $R_{c,0.75,\alpha=0.8}$ do not differ, according to the K-S and sign tests.

TABLE 4

Cluster Core Radii

Name (1)	$R_{c,0.50,\alpha=0.8}$ (2)	$P_{0.50,\alpha=0.8}$ (3)	$R_{c,0.75,\alpha=0.8}$ (4)	$P_{0.75,\alpha=0.8}$ (5)
ACO 85	0.29 ± 0.34	0.94	0.29 ± 0.15	1.00
ACO 119	0.07 ± 0.06	0.74	0.12 ± 0.07	0.79
ACO 151	...	...	...	...
ACO 193	...	...	...	...
ACO 194	0.24 ± 0.17	0.85	0.17 ± 0.08	0.37
ACO 262	0.06 ± 0.06	0.97	0.06 ± 0.05	0.99
ACO 399	...	...	0.41 ± 0.22	0.65
ACO 400	0.13 ± 0.07	0.90	0.12 ± 0.06	0.97
ACO 401	0.10 ± 0.08	0.74	0.15 ± 0.08	0.86
ACO 426/Perseus	0.11 ± 0.05	0.75	0.08 ± 0.04	0.22
ACO 458	0.34 ± 0.42	1.00	...	...
ACO 496	0.28 ± 0.40	0.96	0.19 ± 0.11	0.90
ACO 539	0.05 ± 0.03	0.95	0.05 ± 0.03	0.79
ACO 548	...	...	...	...
ACO 576	0.10 ± 0.05	0.31	...	...
ACO 634	...	...	0.64 ± 0.38	0.90
ACO 744	0.03 ± 0.02	0.54	0.02 ± 0.02	0.18
ACO 754	0.31 ± 0.42	0.96	0.21 ± 0.11	0.22
ACO 779	...	...	...	...
ACO 957	0.06 ± 0.03	0.67	...	...
ACO 999	...	...	0.13 ± 0.08	0.17
ACO 1016	0.08 ± 0.05	0.47	...	...
ACO 1060/Hydra	0.15 ± 0.06	0.71	0.17 ± 0.06	0.62
ACO 1142	...	...	...	...
ACO 1146	0.28 ± 0·29	0·94	0·14 ± 0·06	0·13
ACO 1185	...	...	...	...
ACO 1367	0.14 ± 0.07	0.38	0.12 ± 0.05	0.45
ACO 1631	0.20 ± 0.24	1.00	0.33 ± 0.29	1.00
ACO 1644	0.78 ± 0.36	0.72	0.34 ± 0.21	0.41
ACO 1651	...	...	0.07 ± 0.04	0.84
ACO 1656/Coma	0.10 ± 0.03	0.84	0.08 ± 0.03	0.22
ACO 1736	...	...	...	...
ACO 1736	0.40 ± 0.41	0.77	0.37 ± 0.25	0.69
ACO 1750	0.10 ± 0.06	0.25	0.11 ± 0.06	0.55
ACO 1795	0.17 ± 0.11	0.99	0.20 ± 0.09	0.97
ACO 1809	0.16 ± 0.09	0.85	0.12 ± 0.06	0.19
ACO 1983	0.32 ± 0.35	0.67	0.21 ± 0.10	0.41
ACO 1991	...	...	...	...
ACO 2029	...	...	...	...
ACO 2052	0.09 ± 0.07	1.00	0.08 ± 0.05	0.98
ACO 2063	0.06 ± 0.03	0.66	0.06 ± 0.03	0.54
ACO 2079	...	...	...	...
ACO 2107	0.07 ± 0.03	0.98	0.06 ± 0.03	0.94
ACO 2124	0.20 ± 0.12	0.99	0.13 ± 0.06	0.31
ACO 2147−2152	...	...	...	...
ACO 2151/Hercules	0.28 ± 0.39	0.83	0.29 ± 0.16	0.95
ACO 2197	0.30 ± 0.45	0.77	0.18 ± 0.15	0.62
ACO 2199	...	...	...	...
ACO 2255	...	...	0.03 ± 0.03	0.44
ACO 2256	0.11 ± 0.06	0.98	0.10 ± 0.05	0.84
ACO 2319A	...	...	0.04 ± 0.03	0.97
ACO 2440	0.08 ± 0.06	0.99	...	...
ACO 2538	0.12 ± 0.08	0.81	0.11 ± 0.06	0.83
ACO 2554	0.23 ± 0.19	0.53	...	...
ACO 2589	...	...	...	...
ACO 2593	0.05 ± 0.03	0.40	...	...
ACO 2670	0.12 ± 0.04	0.14	0.12 ± 0.03	0.19
ACO 2717	0.07 ± 0.05	0.69	0.06 ± 0.03	0.48
ACO 2721	0.27 ± 0.28	1.00	0.22 ± 0.12	0.86
ACO 2877	0.09 ± 0.03	0.81	...	...
ACO 3266	0.20 ± 0.13	0.84	0.50 ± 0.35	0.57
ACO 3334	0.09 ± 0.06	1.00	...	...
ACO 3360	0.15 ± 0.08	0.58	...	...
ACO 3376	0.50 ± 0.40	0.81	0.21 ± 0.12	0.60
ACO 3381	...	...	0.16 ± 0.11	0.14
ACO 3389	0.05 ± 0.03	0.83	...	...
ACO 3391	0.24 ± 0.19	1.00	0.23 ± 0.13	0.62
ACO 3395	0.22 ± 0.10	0.56	0.25 ± 0.09	0.71
ACO 3526/Centaurus	0.31 ± 0.19	0.85	0.22 ± 0.08	0.43
ACO 3532	0.06 ± 0.06	0.12	...	...
ACO 3558	0.09 ± 0.03	0.34	0.09 ± 0.03	0.34

TABLE 4—*Continued*

Name (1)	$R_{c,0.50,\alpha=0.8}$ (2)	$P_{0.50,\alpha=0.8}$ (3)	$R_{c,0.75,\alpha=0.8}$ (4)	$P_{0.75,\alpha=0.8}$ (5)
ACO 3574	0.24 ± 0.24	0.88	0.20 ± 0.13	0.75
ACO 3667	0.37 ± 0.41	0.95	0.40 ± 0.30	0.99
ACO 3705	0.55 ± 0.38	0.97	0.19 ± 0.10	0.11
ACO 3716	0.15 ± 0.09	0.79	0.12 ± 0.06	0.49
ACO 3854	0.39 ± 0.42	0.96	0.18 ± 0.11	0.36
ACO 4067	...	...	0.20 ± 0.21	0.96
AWM 1	...	...	...	...
Cancer	0.26 ± 0.32	0.99	0.23 ± 0.14	1.00
DC 0003−50	...	...	0.25 ± 0.19	0.31
Eridanus	...	...	...	...
MKW 4	0.04 ± 0.03	0.99	0.03 ± 0.02	0.68
Pegasus I	...	...	0.11 ± 0.09	0.85
ACO S301	...	...	0.07 ± 0.06	0.47
ACO S373/Fornax	0.08 ± 0.06	0.90	0.13 ± 0.09	0.56
ACO S463	...	...	...	...
S753	0.14 ± 0.13	0.90	0.15 ± 0.10	0.97
ACO S805	...	...	...	...
Ursa Major	...	...	0.68 ± 0.35	0.63
Virgo	0.42 ± 0.32	0.76	0.35 ± 0.11	0.64

This suggests that our estimates of the core radii are quite stable within half an Abell radius.

In order to detect a possible effect of subclustering on the radii estimates, we considered the subsample of our clusters with $N \geq 40$ members (for the reasons outlined in § 2). On this sample we compared the distributions of R_c (and R_v) for clusters with and without evidence of subclustering: there is no difference, according to the K-S test. We caution that this result can be considered neither general, since our cluster sample is not volume complete, nor conclusive, since different tests for subclustering may yield different results (see, e.g., West & Bothun 1990). In fact, a detailed analysis of 16 well-sampled clusters (Escalera et al. 1994) has shown that the estimates of cluster virial radii do decrease when galaxies belonging to subclusters are identified and removed from the sample. However, the changes are not statistically significant in most cases, being important only when the cluster has a *bimodal* configuration, and this happens for only four out of the 16 clusters considered. In most cases the masses of the substructure are $\sim 10\%$ of their parent cluster masses, so it is not surprising that subclustering does not have a very large influence on the size determination.

The analysis of the errors of R_v and R_c suggests that the dispersion of the values of R_v and R_c is partially intrinsic, and not mainly induced by the errors involved.

4.1. *Core Radii versus Virial Radii, and Other Relations*

Both the core and the virial radii describe the galaxy distribution inside the cluster, so the existence of a relation between these two quantities is quite natural. This functional dependence can be easily derived when one knows the density profile.

On the hypothesis that the models we use fit cluster density distributions, we obtain the following relation

$$R_v = R_c\, F(A/R_c) , \qquad (3)$$

where A is the aperture considered. See the Appendix for details.

In our data sample the values obtained for the core and virial radii are very well correlated, at the $>99.99\%$ significance level, for both the apertures of 0.5 and 0.75 h^{-1} Mpc. Figure 1*a* shows log $R_{c,0.5,\alpha=0.8}$ versus log $R_{v,0.5}$, and Figure 1*b* shows log $R_{c,0.75,\alpha=0.8}$ versus log $R_{v,0.75}$. This correlation is not induced by obvious observational biases (i.e., the radii do not correlate with the cluster distance, or with the number of cluster members we use, etc.). These relations remain practically unchanged if clusters with significant subclustering are removed. The theoretical curves derived from equation (3) are superimposed on the data in Figure 1.

As can be seen, the observational relations between core and virial radii are in good agreement with the respective theoretical relations, described via equation (3) and obtained with our ($\alpha = 0.8$) profiles. This strongly supports the choice of these profiles in the description of cluster density distributions.

Moreover, it is possible to compare the measured R_v with the corresponding values $R_{v,\mathrm{comp}}$ computed from the observed R_c and the respective apertures using equation (3). R_v correlates with $R_{v,\mathrm{comp}}$ at a significance level higher than 99.99%. For the virial radii the regression bisector line (see, e.g., Isobe et al. 1990) is

$$R_{v,0.75,\mathrm{comp}} = 0.02(\pm 0.04) + 0.96(\pm 0.06) R_{v,0.75} . \qquad (4)$$

Figure 2 shows $R_{v,0.75,\mathrm{comp}}$ versus $R_{v,0.75}$. Obviously, it is also possible to compare the measured R_c with the corresponding values $R_{c,\mathrm{comp}}$ computed from the observed R_v and the respective apertures using equation (3), and the result is quite similar.

As a consequence of this analysis, since the estimate of R_v is usually more straightforward than that of R_c, one can evaluate R_c when R_v and the corresponding aperture are known.

We also investigated the existence of a correlation between R_v (and R_c) and other optical cluster quantities, such as the Abell richness, the morphological types by Bautz-Morgan and by Rood-Sastry, as reported in Table 1, and the robust velocity dispersions computed as in GBGMM: we found no strong evidence of correlation.

The comparison between optical and X-ray core radii has been extensively discussed with controversial results (see, e.g., Lea et al. 1973; Smith, Mushotzky, & Serlemitos 1979; Abramapoulous & Ku 1983). Detailed optical analysis of few clusters (see, e.g., Ku et al. 1983; Henry & Henriksen 1986) suggest that optical and X-ray core radii are comparable within observational errors (see also David et al. 1990). We considered the X-ray core radii, R_x, of Jones & Forman (1984); the median value of α in their fits is $\sim 0.7 \pm 0.1$, which agrees with our

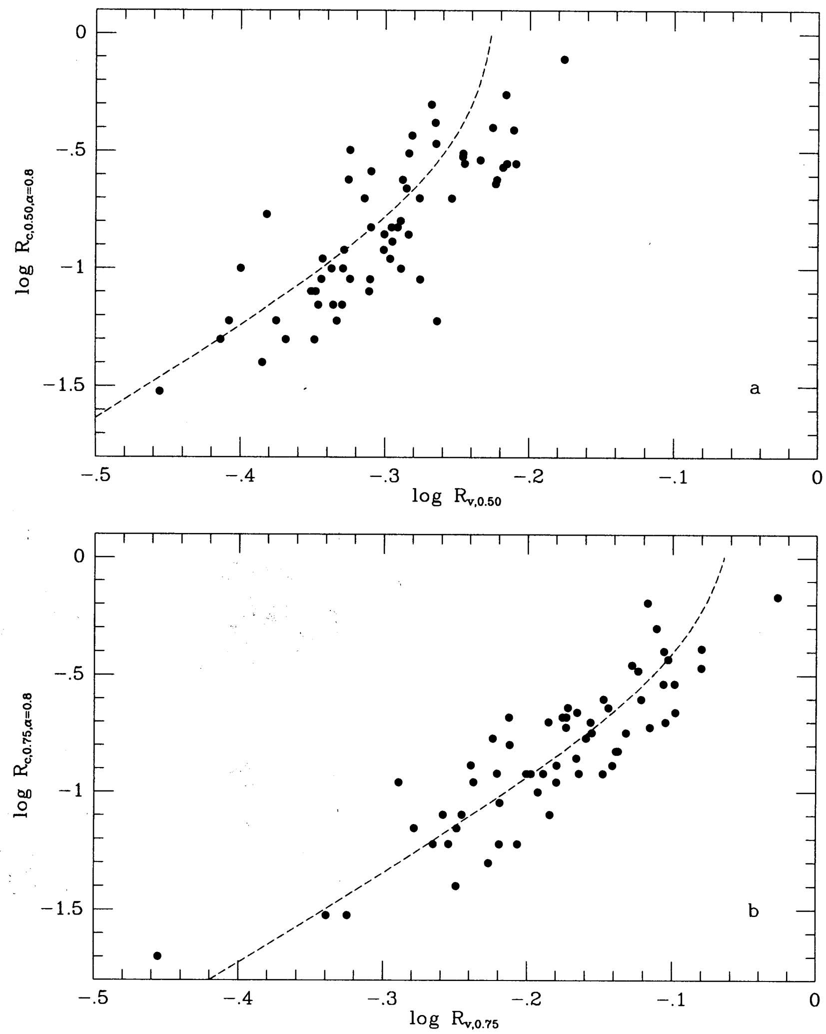

FIG. 1.—(*a*) log $R_{c,0.5,\alpha=0.8}$ vs. log $R_{v,0.5}$ and (*b*) log $R_{c,0.75,\alpha=0.8}$ vs. log $R_{v,0.75}$. The superimposed curves are derived from eq. (3).

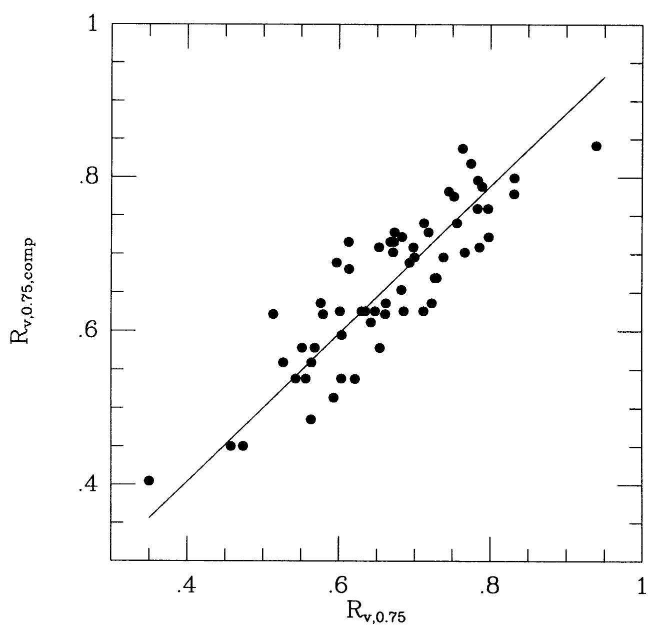

FIG. 2.—$R_{v,comp}$ vs. R_v. The superimposed regression line (eq. [4]) does not significantly differ from the bisector line.

optical $\alpha = 0.8$. The distribution function of R_x does not differ (according to the K-S test) from that of our $R_{c,0.75,\alpha=0.8}$, when the common subsample of 18 clusters is considered. Figure 3 shows these distributions.

4.2. *Radii Distributions*

Our cluster set is not volume complete. Therefore, in order to estimate the cosmic distributions for our cluster core and virial radii, we should normalize our observational distributions to a complete cluster sample. For this purpose, we considered the Cluster Catalogue of Abell, Corwin, & Olowin (1989, hereafter ACO), which is nominally complete for clusters with redshift $z \leq 0.2$ and richness class $R \geq 1$.

In GBGMM and Biviano et al. (1993) we used the Abell richness distribution to normalize the distributions of cluster velocity dispersions and, respectively, of cluster virial masses. The normalization makes sense because the richnesses are available for all ACO clusters, and both velocity dispersion and virial mass correlate with richness. Since there is no significant correlation between cluster size and richness, it is not obvious that a similar normalization would work in this case. On the other hand, the same lack of correlation suggests that the cluster size distribution should not depend critically on

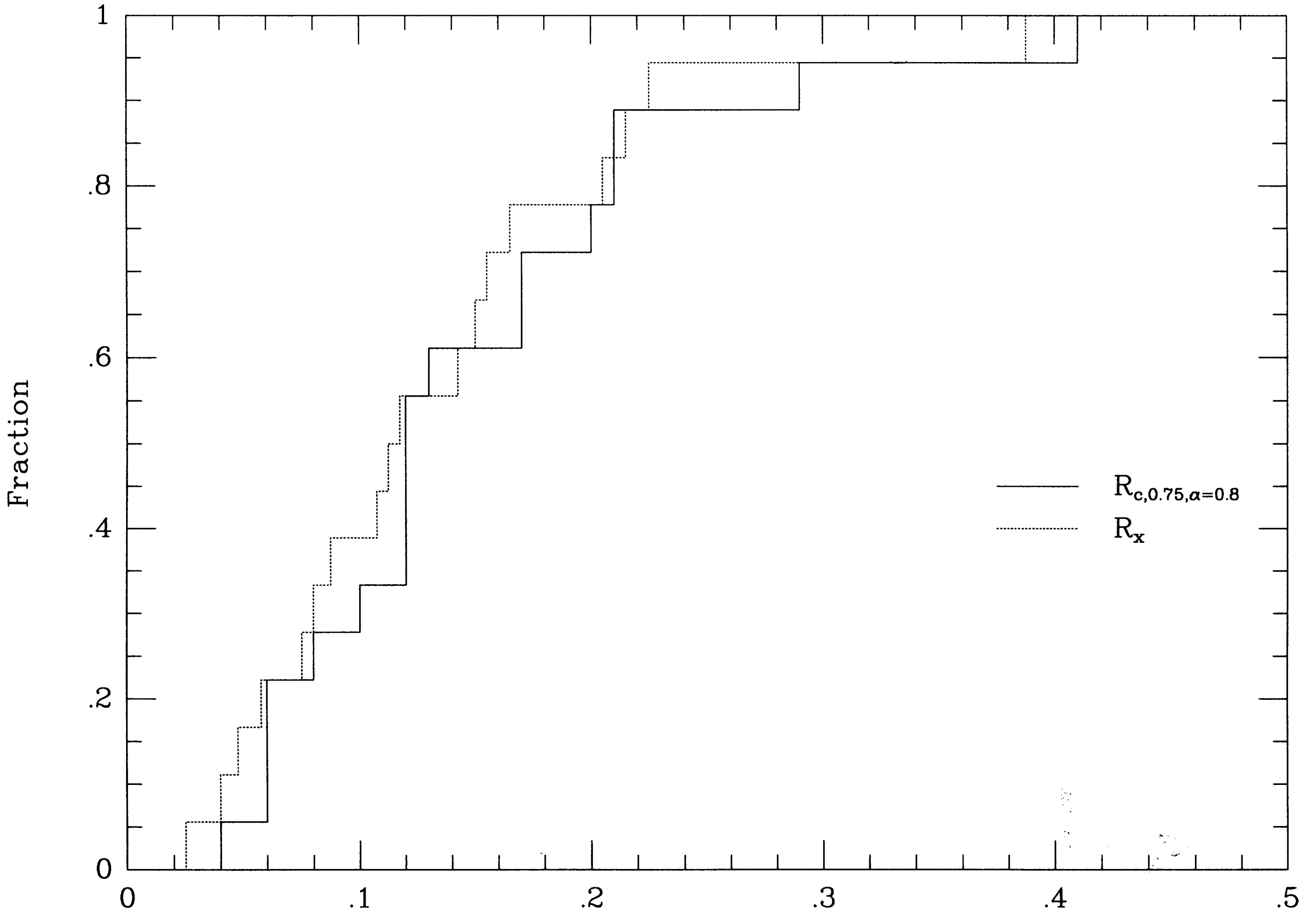

FIG. 3.—Cumulative distributions of $R_{c,0.75,\alpha=0.8}$ (*solid line*) and of the X-ray core radii of Jones & Forman (1984) (*dotted line*) for the common subsample of clusters.

completeness. We decided to perform the normalization to richness, anyway.

The normalization was accomplished by randomly extracting 1000 values of R_c and R_v from the corresponding values measured in our clusters, in such a way as to reproduce the richness distribution of ACO's cluster sample (poor sample statistics forced us to consider clusters with $R \geq 3$ as belonging to the same class).

We considered the values of $R_{c,0.75,\alpha=0.8}$, listed in Table 4, having excluded the $R = 0$ clusters (ACO is complete for $R \geq 1$). The corresponding ACO-normalized cumulative distributions are shown in Figure 4; the median value of this distribution is $0.17^{+0.04}_{-0.05}$ h^{-1} Mpc (where the 99% interval limits of the median are indicated).

Since the virial radii depend on the apertures used, we cannot provide a single cosmic distribution of virial radii. So, we chose the aperture 0.75 h^{-1} Mpc (half an Abell radius) and the values of $R_{v,0.75}$ given in Table 2. The ACO-normalized cumulative distributions for $R_{v,0.75}$ are shown in Figure 5. The median value (with 99% interval limits) is $0.67^{+0.04}_{-0.06}$ h^{-1} Mpc.

5. CONCLUSIONS

The cluster sample considered here is the most extensive one in the literature for the evaluation of virial radii and the fitting of galaxy density profiles, but it is not volume complete.

Most of our cluster profiles (~90%) are fitted by hydrostatic isothermal-like profiles with $\alpha = 0.8$; this result is, therefore, quite general.

Our optical results are consistent with the hypothesis that many clusters, within the errors and the apertures considered, are satisfactorily described by isothermal models. In fact, the slope of our best-fit profiles is similar to that of X-ray cluster profiles (e.g., Jones & Forman 1984). Therefore we agree with the analysis of Bahcall & Lubin (1993), who suggested a value of $\alpha = 0.7 \pm 0.1$ in order to resolve the β-discrepancy.

This result may seen surprising in view of the mounting evidence that subclustering is ubiquitous in clusters (see, e.g., Bird 1994). However, as discussed by West (1990), evidence for subclustering does not necessarily imply dynamical youth for the cluster. Classical tests for subclustering do not make any distinction between the case of simple geometrical projection of a group onto a cluster field, the case of a group that is falling into an otherwise relaxed cluster, and the case of real substructure, i.e., a true perturbation of the cluster dynamical potential. Moreover, subcluster masses are often an order of magnitude lower than their parent cluster masses (Escalera et al. 1994), and therefore their influence on the main cluster properties need not to be huge.

Our virial radii correlate with our core radii at a very high significance level. The relationship between these two size estimates obeys the theoretical relationship which links the virial radius to the density profile with $\alpha = 0.8$.

We provide the distribution functions of R_v and R_c obtained within a fixed aperture of half an Abell radius. The analysis of the radius errors allows us to claim that the dispersion of the values of the cluster radii is partially intrinsic. The median

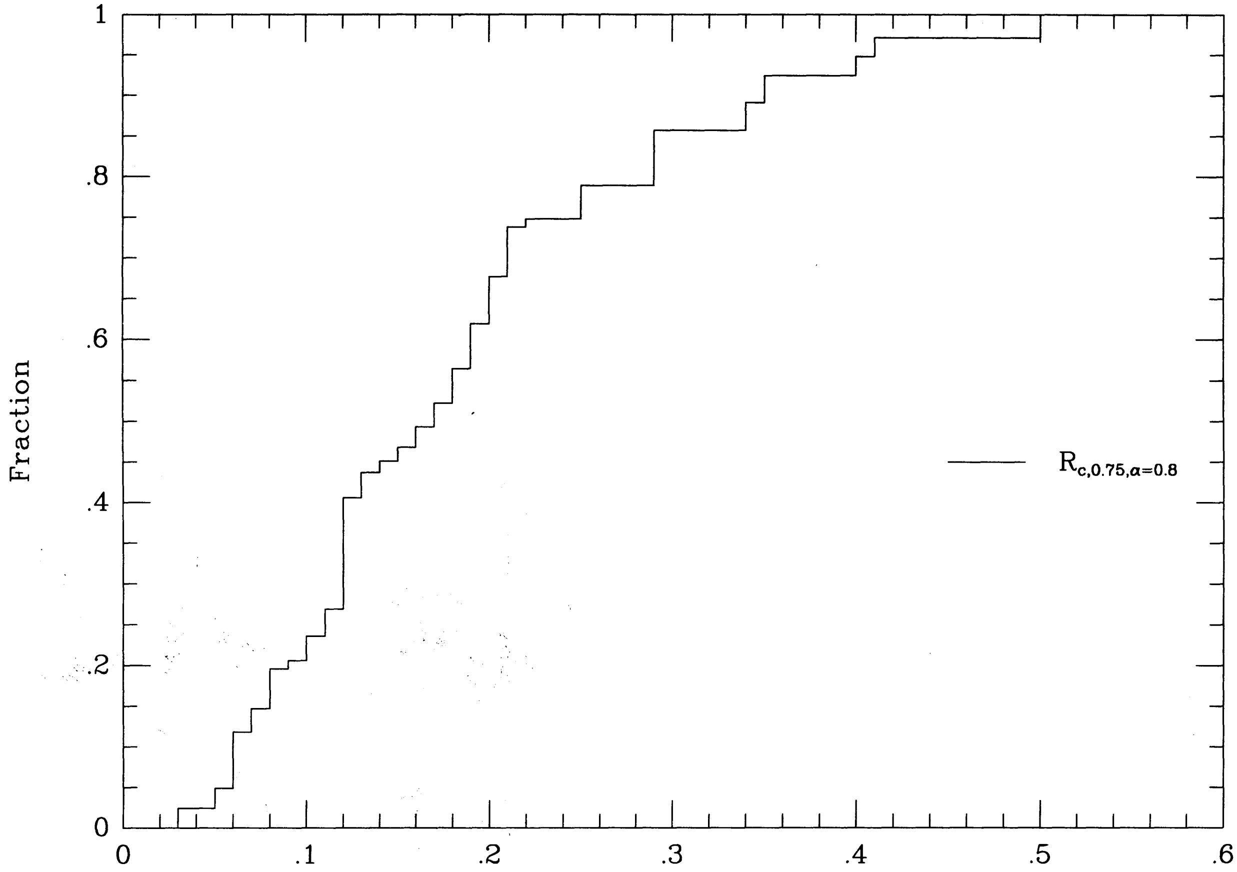

FIG. 4.—ACO-normalized cumulative distribution of the core radii

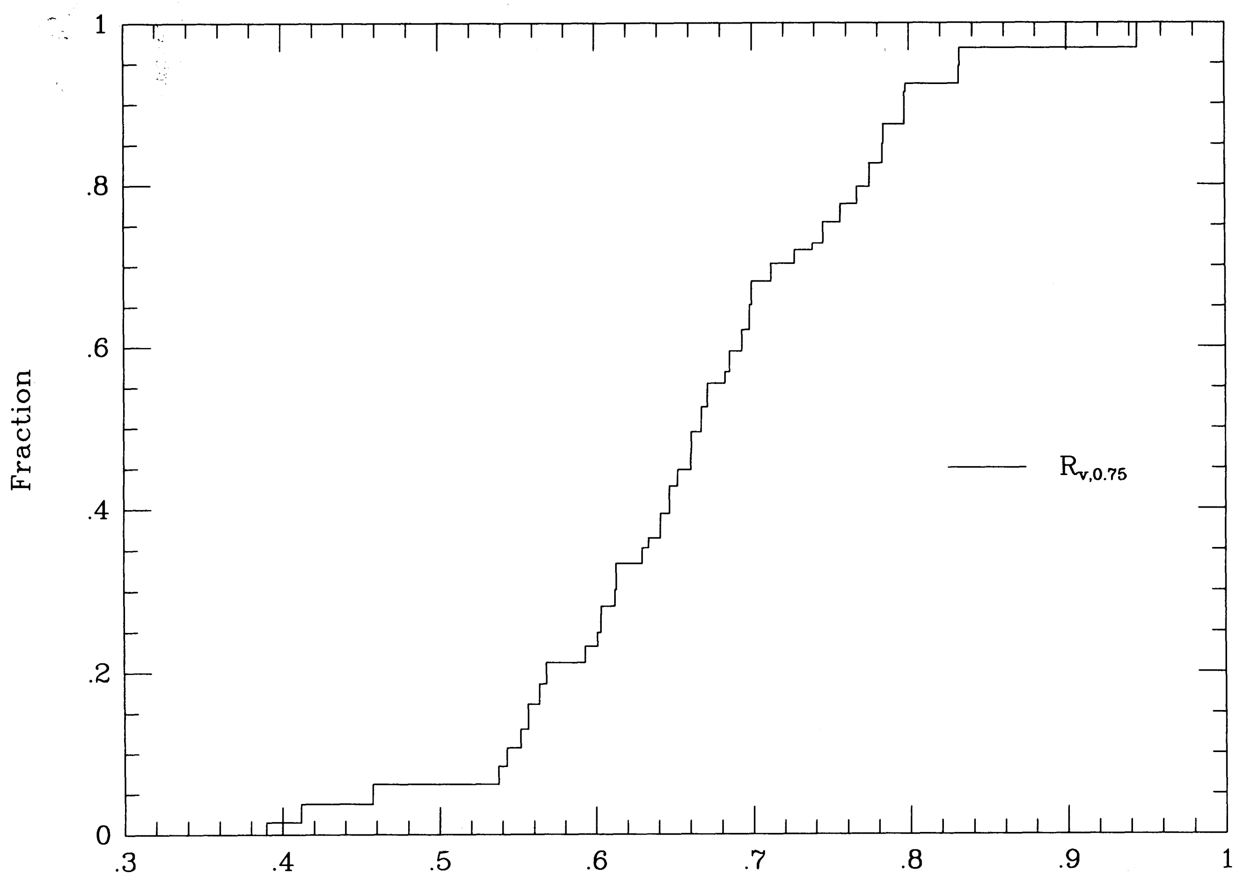

FIG. 5.—ACO-normalized cumulative distribution of the virial radii, evaluated within half an Abell radius.

value of our core radii is 0.17 h^{-1} Mpc, and the median value of our virial radii (within half an Abell radius) is 0.67 h^{-1} Mpc.

We thank C. Sarazin for kindly providing us with his FORTRAN code for the maximum likelihood analysis of density profiles, J. Hill for giving us an electric copy of his cluster data, and M. West, the referee, for his useful suggestions. This work was partially supported by the Ministero per l'Università e per la Ricerca scientifica e tecnologica, and by the Consiglio Nazionale delle Ricerche (CNR-GNA).

APPENDIX

Both our core and virial radii (R_c and R_v, respectively) describe the galaxy distribution inside the cluster, so the existence of a relation between these two quantities is quite natural. This functional dependence can be derived when one knows the density profile.

The three-dimensional virial radius $R_{v,3D}$ of a distribution of N cluster galaxies of masses m_i on the sky plane, within a circular aperture of radius A, is given by the usual relation expressing the total potential energy of the system. Since only projected positions are known for the galaxies, a deprojection factor (usually $\pi/2$) is used to deduce $R_{v,3D}$ from its projected value R_v, which is derived from the relation

$$-\frac{G}{R_v}\left(\sum_{i=1}^{N} m_i\right)^2 = -G \sum_{\substack{i,j=1 \\ i \neq j}}^{N} \frac{m_i m_j}{R_{ij}}, \tag{A1}$$

which becomes our equation (2) on the hypothesis that galaxy masses do not correlate with galaxy positions in clusters. This hypothesis is largely assumed in the literature, and it is justified by the absence of pronounced luminosity segregation in galaxy clusters (see, e.g., Biviano et al. 1992).

The relation (A1) describes the total potential energy of the two-dimensional distribution of masses. It is thus possible to evaluate R_v for a given surface density profile $\sigma(r/R_c)$ ($r \leq A$), knowing the total potential energy $W_{2D}(A)$ of the disk of radius A. This energy is

$$W_{2D}(A) = \tfrac{1}{2} 2\pi \int_0^A \Phi(r)\sigma(r/R_c) r \, dr \; ; \tag{A2}$$

in equation (A2) the factor 1/2 avoids counting twice the same couples of mass elements in the disk, and the gravitational potential $\Phi(r)$ (using polar coordinates (r', ϕ)) is

$$\Phi(r) = -G \int_0^A \int_0^{2\pi} \frac{\sigma(r'/R_c) r'}{r^2 + r'^2 - 2rr' \cos\phi} \, d\phi \, dr' = -GR_c \, I\left(\frac{r}{R_c}\right). \tag{A3}$$

The function $I(r/R_c) = I(x)$ (where $x = r/R_c$) may be expressed, using the complete elliptical integral of first kind $K(y)$ (see Binney & Tremaine 1987, p. 73), as

$$I(x) = 4 \int_0^{A/R_c} \frac{\sigma(u) u}{x + u} K\left[\frac{4ux}{(u+x)^2}\right] du \, , \tag{A4}$$

where $u = r'/R_c$ and $K(y)$ is defined by

$$K(y) = \int_0^1 \frac{dt}{\sqrt{[(1-t^2)(1-yt^2)]^{1/2}}} \, . \tag{A5}$$

From these relations it is possible to obtain the relation between R_v and R_c, for a given profile and aperture:

$$R_v = R_c \frac{4\pi [\int_0^{A/R_c} \sigma(x) x \, dx]^2}{\int_0^{A/R_c} I(x)\sigma(x) x \, dx} = R_c \, F\left(\frac{A}{R_c}\right). \tag{A6}$$

The function $F(A/R_c)$ can be evaluated for any given surface density profile $\sigma(r/R_c)$. For the profile

$$\sigma\left(\frac{r}{R_c}\right) = \frac{\sigma_0}{[1 + (r/R_c)^2]^{0.8}} \, . \tag{A7}$$

$F(A/R_c)$ is well represented, for $0.01 \leq (A/R_c) \leq 100$ and with an accuracy better than 3%, by the relation

$$F\left(\frac{A}{R_c}\right) = 1.193\left(\frac{A}{R_c}\right) \frac{1 + 0.032(A/R_c)}{1 + 0.107(A/R_c)} \, . \tag{A8}$$

REFERENCES

Abell, G. O., Corwin, H. G., Jr., & Olowin, R. P. 1989, ApJS, 70, 1 (ACO)
Abramopoulous, F., & Ku, W. H. 1983, ApJ, 271, 446
Avni, Y. 1976, 210, 642
Bahcall, N. A. 1975, ApJ, 198, 249
———. 1977, ARA&A, 15, 505
Bahcall, N. A., & Lubin, L. M. 1993, ApJ, 415, L17
Beers, T. C., Gebhardt, K., Huchra, J. P., Forman, W., Jones, C., & Bothun, G. D. 1992, ApJ, 400, 410
Beers, T. C., Geller, M. J., Huchra, J. P., Latham, D. W., & Davis, R. J. 1984, ApJ, 283, 33

Beers, T. C., Flynn, K., & Gebhardt, K. 1990, AJ, 100, 32
Beers, T. C., Forman, W., Huchra, J. P., Jones, C., & Gebhardt, K. 1991, AJ, 102, 1581
Bell, M., & Whitmore, B. C. 1989, ApJS, 70, 139
Binggeli, B., Sandate, A., & Tammann, G. A. 1985, AJ, 90, 1681
Binney, J., & Tremaine, S. 1987, Galactic Dynamics (Princeton: Princeton Univ. Press)
Bird, C. 1994, preprint
Biviano, A., Girardi, M., Giuricin, G., Mardirossian, F., & Mezzetti, M. 1992, ApJ, 396, 35
———. 1993, ApJ, 411, L13
Bothun, G. D., Aarsonson, M., Schommer, B., Mould, J., Huchra, J., & Sullivan, W. T., III 1985, ApJS, 57, 423
Bothun, G. D., Geller, M. J., Beers, T. C., & Huchra, J. P. 1983, ApJ, 268, 47
Bowers, R. G., Ellis, R. S., & Efstathiou, G. 1988, MNRAS, 234, 725
Cavaliere, A., Colafrancesco, S., & Scaramella, R. 1991, ApJ, 380, 15
Chapman, G. N. F., Geller, M. J., & Huchra, J. P. 1987, AJ, 94, 571
———. 1988, AJ, 95, 999
Chincarini, G., & Rood, H. J. 1976, PASP, 88, 388
Colless, M., & Hewett, P. 1987, MNRAS, 224, 453
Cristiani, S., de Souza, R., D'Odorico, S., Lund, G., & Quintana, H. 1987, A&A, 179, 108
David, L. P., Arnaud, K. A., Forman, W., & Jones, C. 1990, ApJ, 356, 32
Dickens, R. J., Currie, M. J., & Lucey, J. R. 1986, MNRAS, 220, 679
Dickens, R. J., & Moss, C. 1976, MNRAS, 174, 47
Dressler, A. 1978, ApJ, 226, 55
Dressler, A., & Shectman, S. A. 1988a, AJ, 95, 284
———. 1988b, AJ, 95, 985
Durret, F., Gerbal, D., Lachièze-Rey, M., Lima-Neto, G., & Sadat, R. 1994, A&A, 287, 733
Edge, A. C., & Stewart, G. C. 1991, MNRAS, 252, 428
Efron, B. 1979, SIAM Rey., 21, 460
Escalera, E., Biviano, A., Giradi, M., Giuricin, G., Mardirossian, F., Mazure, A., & Mezzetti, M. 1994, ApJ, 423, 539
Eyles, C. J., Watt, M. P., Bertram, D., Church, M. J., Ponma, T. J., Skinner, G. K., & Willmore, A. P. 1991, ApJ, 376, 23
Faber, S. M., & Dressler, A. 1977, AJ, 82, 187
Fabricant, D. G., Kent, S. M., & Kurtz, M. J. 1989, ApJ, 336, 77
Fabricant, D., Kurtz, M., Geller, M., Zabludoff, A., Mack, P., & Wegner, G. 1993, AJ, 105, 788
Fernley, J. A., & Bhavsar, S. P. 1984, MNRAS, 210, 883
Fitchett, M.-J., Merritt, D. 1988, ApJ, 335, 18
Gavazzi, G. 1987, ApJ, 320, 96
Geller, M. J. 1984, in Clusters and Groups of Galaxies, ed. F. Mardirosssian, G. Giuricin, & M. Mezzetti (Dordrecht: Reidel), 353
Geller, M. J., Beers, T. C., Bothun, G. D., & Huchra, J. P. 1984, AJ, 89, 319
Gerbal, D., Durret, F., & Lachièze-Rey, M. 1994, A&A, in press
Gerbal, D., Durret, F., Lima-Neto, G., & Lachièze-Rey, M. 1992, A&A, 253, 77
Giovanelli, R., Haynes, M. P., & Chincarini, G. L. 1982, ApJ, 262, 442
Giradi, M., Biviano, A., Giuricin, G., Mardirossian, F., & Mezzetti, M. 1993, ApJ, 404, 38 (GBGMM)
Giuricin, G., Mardirossian, F., & Mezzetti, M. 1984, A&A, 141, 419
Gregory, S. A., & Thompson, L. A. 1978, ApJ, 222, 784
———. 1984, ApJ, 286, 422
Gregory, S. A., Thompson, L. A., & Tifft, W. G. 1981, ApJ, 243, 411
Henry, J. P., & Henriksen, M. J. 1986, ApJ, 301, 689
Hill, J. M., & Oegerle, W. R. 1993, AJ, 106, 831
Hintzen, P., Hill, J. M., Lindley, D., Scott, J. S., & Angel, J. R. P. 1982, AJ, 87, 1656
Hintzen, P., Oegerle, W. R., & Scott, J. S. 1978, AJ, 83, 478
Inagaki, S., Itoh, M., & Saslaw, W. C. 1992, ApJ, 386, 9
Isobe, T., Feigelson, E. D., Akritos, M. G., & Babu, G. J. 1990, ApJ, 364, 104
Jones, C., & Forman, W. 1984, ApJ, 276, 38
———. 1992, in Clusters and Superclusters of Galaxies, ed. A. C. Fabian (Dordrecht: Kluwer), 49
Kashlinsky, A. 1992, ApJ, 386, L37
Kent, S. M., & Gunn, J. E. 1982, AJ, 87, 945
Kent, S. M., & Sargent, W. L. W. 1983, AJ, 88, 697
King, I. R. 1962, AJ, 67, 471
———. 1966, AJ, 71, 64
Kneib, J.-P., Mellier, Y., Fort, B., & Mathez, G. 1993, A&A, 273, 367
Ku, W. F., Abramopoulos, F., Nulsen, P. E. J., Fabian, A. C., Stewart, G. C., Chincarini, G., & Tarenghi, M. 1983, MNRAS, 203, 253
Kurtz, M. J., Huchra, J. P., Beers, T. C., Geller, M. J., Gioia, I. M., Maccacaro, T., Schild, R. E., & Stauffer, J. R. 1985, AJ, 90, 1665
Lauberts, A., & Valentjin, E. A. 1989, The Surface Photometry Catalogue of the ESO-Uppsala Galaxies (Garching bei München: ESO)
Lea, S., Silk, J., Kellogg, E., & Murray, S. 1973, ApJ, 184, L105
Lilje, P. B., & Lahav, O. 1991, ApJ, 374, 29
limber, D. N., & Matthews, W. G. 1960, ApJ, 1232, 286
Lubin, L. M., & Bahcall, N. A. 1993, ApJ, 415, L17
Lynden-Bell, D. 1967, MNRAS, 136, 101
Malumuth, E. M., & Kriss, G. A. 1986, ApJ, 308, 10
Malumuth, E. M., Kriss, G. A., Van Dyke Dixon, W., Ferguson, H. C., & Ritchie, C. 1992, AJ, 104, 495
Metcalfe, N., Godwin, J. G., & Spenser, S. D. 1987, MNRAS, 225, 581
Miralda-Escudé, J. 1992, ApJ, 390, L65
Moss, C., & Dickens, R. J. 1977, MNRAS, 178, 701
Oegerle, W. R., & Hill, J. M. 1993, AJ, 104, 2078
Oemler, A., Jr. 1974, ApJ, 194, 1
Ostriker, E. C., Huchra, J. P., Geller, M. J., & Kurtz, M. J. 1988, AJ, 96, 177
Peebles, P. J. 1970, AJ, 75, 13
———. 1976, ApJ, 205, L109
Peebles, P. J., Daly, R. A., & Juszkiewicz, R. 1989, ApJ, 347, 563
Perea, J., Del Olmo, A., & Moles, M. 1990, A&A, 237, 319
Pisani, A., Giuricin, G., Mardirossian, F., & Mezzetti, M. 1992, ApJ, 389, 68
Postman, M., Huchra, J. P., & Geller, M. J. 1986, AJ, 92, 1238
Proust, D., Quintana, H., Mazure, A., da Souza, R., Escalera, E., Sodrè, L., Jr., & Capelato, H. V. 1992, A&A, 258, 243
Quintana, H., Melnick, J., Infante, L., & Thomas, B. 1985, AJ, 90, 410
Quintana, H., & Ramirez, A. 1990, AJ, 100, 1424
Rhee, G., van Haarlem, M., & Katgert, P. 1992, AJ, 103, 1721
Richter, O. G. 1987, A&AS, 67, 237
———. 1989, A&AS, 77, 237
Richter, O. G., & Huchtmeier, W. K. 1982, A&A, 109, 155
Sarazin, C. L. 1980, ApJ, 236, 75
———. 1986, Rev. Mod. Phys., 58, 1
Sharples, R. M., Ellis, R. S., & Gray, P. M. 1988, MNRAS, 231, 479
Smith, B. W., Mushotzky, R. F., & Serlemitos, P. J. 1979, ApJ, 227, 37
Smith, H., Jr. 1980, ApJ, 241, 63
Sodrè, L., Capelato, H. V., Steiner, J. E., Proust, D., & Mazure, A. 1992, MNRAS, 259, 233
Soucail, G. 1992, in Clusters and Superclusters of Galaxies, ed. A. C. Fabian (Dordrecht: Kluwer), 199
Stauffer, J., Spinrad, H., & Sargent, W. L. W. 1979, ApJ, 228, 379
Stepanyan, Dzh.A. 1984, Astrophysics, 20, 478
Tarenghi, M., Tifft, W. G., Chincarini, G., Rood, H. J., & Thompson, L. A. 1979, ApJ, 234, 793
Teague, P. F., Carter, D., & Gray, P. M. 1990, ApJS, 72, 715
Tifft, W. G. 1978, ApJ, 222, 54
Tully, R. B. 1988, Nearby Galaxy Catalog (Cambridge: Cambridge Univ. Press)
West, M. J. 1990, in Clusters of Galaxies, ed. W. R. Oegerle & M. J. Fitchett (Cambridge: Cambridge Univ. Press), 65
West, M. S., & Bothun, G. D. 1990, ApJ, 350, 36
West, M. J., Dekel, A., & Oemler, A. 1987, ApJ, 316, 1
West, M. J., Oemler, A., & Dekel, A. 1989, ApJ, 327, 1
Willmer, C. N. A., Focardi, P., Chan, R., Pellegrini, P. S., & Nicolaci Da Costa, L. 1991, AJ, 101, 57
Willmer, C. N. A., Focardi, P., Nicolaci Da Costa, L., & Pellegrini, P. S. 1989, AJ, 98, 1531
Zabludoff, A. I., Huchra, J. P., & Geller, M. J. 1990, ApJS, 74, 1